Intersubband resonant scattering in GaAs-$Ga_{1-x}Al_xAs$ heterojunctions

D. R. Leadley, R. Fletcher,* and R. J. Nicholas
Department of Physics, Clarendon Laboratory, Parks Road, Oxford OX1 3PU, United Kingdom

F. Tao
Department of Physics, Queen's University, Kingston, Ontario, Canada K7L 3N6

C. T. Foxon
Department of Physics, The University, Nottingham NG7 2RD, United Kingdom

J. J. Harris
Semiconductor Interdisciplinary Research Centre, Imperial College, London SW7 2BZ, United Kingdom

(Received 20 January 1992)

Shubnikov–de Haas oscillations have been investigated in the resistivity of three GaAs-$Ga_{1-x}Al_xAs$ heterojunctions, each with two subbands occupied, at temperatures below 4.2 K. As shown in previous publications, oscillations from the lower subband do not conform to the standard theory. The envelope of these oscillations is strongly modulated at the frequency of the upper subband oscillations and, under conditions where the ratio of temperature to magnetic field is large, the oscillations are anomalously large. The oscillations from the upper subband do not exhibit any measurable anomalies. The results are reasonably well explained by a model due to Coleridge which takes into account elastic intersubband scattering. We find that the model predicts that intersubband resonant scattering produces a series of resistivity oscillations which are not damped as the temperature rises. The effect is analogous to magnetophonon resonance in its insensitivity to thermal damping. Hot-electron studies have also been performed, which are qualitatively similar to the cold electron experiments, but differ in that the modulation envelope is shifted in phase by π. This feature cannot be interpreted by a model which takes into account only elastic scattering, and we conclude that it is due to additional inelastic, electron-phonon, intersubband scattering.

I. INTRODUCTION

This paper will discuss the anomalous behavior of Shubnikov–de Haas (SdH) oscillations in GaAs-$Ga_{0.7}Al_{0.3}As$ heterojunctions in which two electric subbands are occupied. The resistivity in such samples is usually expected to show oscillations periodic in inverse magnetic field at two frequencies, f_1 and f_2, arising from the lower and upper subbands, respectively. If there is only one subband the SdH frequency is related to the carrier concentration n by $f=nh/2e$, and since there are far more carriers in the lower subband $f_1 \gg f_2$. Typical traces are shown in Fig. 1 for two of the samples discussed in this paper, in which f_1 is approximately 10 times greater than f_2. We will demonstrate that, at low magnetic fields and high temperatures, the simple picture of two independent series breaks down and the oscillations become dominated by a scattering term which has a new periodicity f_1-f_2, and does not show the usual temperature-dependent damping characteristic of SdH oscillations.

Several aspects of this anomalous behavior have been reported previously.[1–3] Leadley *et al.*[1] first noticed that the amplitude of the oscillations at f_1 was strongly modulated at the frequency f_2. At the lowest temperatures this modulation was modest but it increased with temperature with the striking result that the amplitude of the f_1 oscillations sometimes passed through zero. Because the effect increased with temperature and was strongly linked to the upper subband oscillations, it was

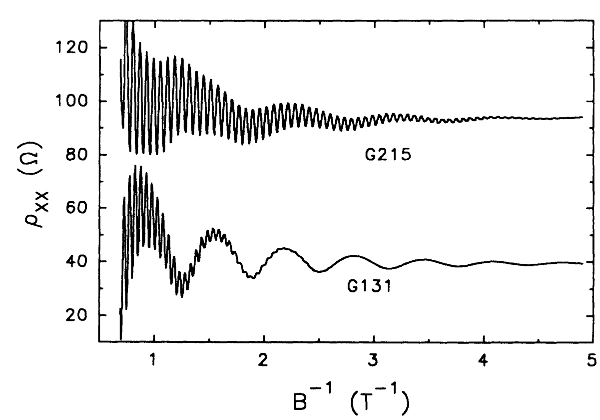

FIG. 1. The resistivity of samples G131 and G215 at 0.55 K as a function of inverse magnetic field. The data for sample G215 have been offset vertically by 80 Ω. The low-frequency oscillations have similar amplitudes for the two samples (relative to ρ_0), because their Dingle temperatures T_{D_2} are comparable. The high-frequency oscillations are damped more strongly for sample G131 compared to sample G215 as a result of a much larger T_{D_1}.

tentatively attributed to the effects of acoustic-phonon-mediated intersubband scattering. However, in relatively high mobility heterojunctions the zero-field resistivity ρ_0 is hardly affected by electron-phonon scattering[4] in the temperature region where the SdH oscillations are observed ($T \le 4.2$ K), and so this identification of the mechanism remained controversial.

Later Coleridge[2] published data showing similar effects and developed a model based on elastic intersubband and intrasubband scattering to explain them. Analytic results were evaluated only with the simplifying assumption that the Fermi level remained fixed as the magnetic field varied. The model predicted a modulation, though it appeared that its amplitude should decrease (relative to that of f_1) as the temperature increased, in contrast to the experimental results. However, the results of a single numerical calculation were also presented in which the total carrier density was fixed (a more realistic condition for heterojunctions), where the relative modulation amplitude indeed increased with temperature. We believe that the difference between the two results is not, in fact, due to fixing the Fermi level, but is caused by the neglect of a resonance effect between the two subbands which was not noticed in the analytic version. This is explained in Sec. II where the model is discussed in more detail.

Anomalous behavior has also been reported in the amplitudes and frequencies of the oscillations by Fletcher, Harris, and Foxon.[3] The standard expression for the oscillatory part of the resistivity $\Delta\rho_{XX}$ of a two-dimensional electron gas (2DEG) due to SdH oscillations of frequency f is[5-7]

$$\Delta\rho_{xx} = 2A\rho_0\Phi(T_D)D(X)\cos(2\pi f/B - \pi) , \quad (1)$$

where $D(X) = X/\sinh X$ is the thermal damping factor, with $X = 2\pi^2 k_B T/\hbar\omega_c$ and ω_c is the cyclotron frequency. (Note that, using $m^* = 0.068 m_e$, X is numerically equal to T/B.) The Dingle factor $\Phi(T_D) = \exp(-2\pi^2 k_B T_D/\hbar\omega_c)$, with the Dingle temperature T_D, incorporates the effect of impurity scattering on the Landau-level widths. The amplitude is written as $2A\rho_0$ for consistency with the development in Sec. II. Fletcher, Harris, and Foxon analyzed their experimental data on the high-frequency oscillations for agreement with Eq. (1). It was found that at low values of X the data were indeed consistent with this equation, but for $k_B T/\hbar\omega_c \ge 0.35$ (i.e., $X \ge 7.0$) they were not. In particular, the experimental data reached amplitudes at least two orders of magnitude larger than predicted. It also appeared that in the anomalous amplitude region the frequency was $f_1 - f_2$ rather than f_1. Both of these features were again tentatively explained in terms of electron-phonon scattering. It should be noted that Coleridge also noticed frequency shifts in his experimental data and ascribed them to frequency modulation due to variations in the Fermi level in his elastic-scattering model.

A possible ways to distinguish elastic and inelastic scattering effects is to compare the oscillations from hot and cold electrons. For cold electrons, thermal equilibrium exists between electrons and lattice, whereas for hot electrons the lattice is cooler than the electrons and phonon emission will dominate. For a given electron temperature the elastic effects will be identical in the two cases since the phonons are not involved.

The present experiments were designed to exploit this idea and have examined the SdH oscillations in three high-mobility $GaAs\text{-}Ga_{1-x}Al_xAs$ heterojunctions with two subbands occupied. It was indeed found that the results were different for hot and cold electrons. The results indicate that there is a competition between elastic and inelastic effects, with the former dominating in the case of cold electrons. In Secs. II and IV we will show how the concept of an intersubband resonance phenomenon (which is implicit in the Coleridge model) explains the observed behavior in the elastic case.

II. THEORY

As mentioned above, the only theory that has so far been advanced to attempt to explain the modulation effect in two band samples is that of Coleridge[2] based on elastic scattering. The restriction to elastic scattering means that its predictions must be the same for both hot and cold electrons at a given electron temperature. Our results show that differences do exist, but these are weakest for the lowest mobility sample in which elastic scattering will be strongest. Furthermore, at sufficiently low temperatures all samples will be dominated by elastic scattering. We examine the predictions of this model in these limiting cases.

With the assumption of a fixed Fermi level the analytic version of the Coleridge model yields a result of the form

$$\frac{\Delta\rho_{xx}}{\rho_0} = A_1\frac{\langle\Delta g_1\rangle}{g_0} + A_2\frac{\langle\Delta g_2\rangle}{g_0} + B_{12}\frac{\langle\Delta g_1\Delta g_2\rangle}{g_2^2} , \quad (2)$$

where g_0 is the density of states (DOS) for a single subband in zero field. The quantities Δg_i are the oscillating parts of the DOS in the ith subband, which, ignoring harmonics, may be written as

$$\frac{\Delta g_i}{g_0} = 2\Phi(T_{D_i})\cos\left\{2\pi\frac{E_F - E_{0i}}{\hbar\omega_c} + \pi\right\} . \quad (3)$$

In this expression T_{D_i} is the appropriate Dingle temperature and E_{0i} the minimum energy of the ith subband. The coefficients A_i and B_{12} are obtained in terms of the probabilities P_{ij} for intrasubband ($i = j$) and intersubband ($i \ne j$) scattering and, if terms in n_2/n_1 (n_i being the electron density in the ith subband) are ignored, one obtains $A_2 \simeq P_{12}/(P_{11}+P_{12}) \simeq B_{12}$ and $A_1 \simeq 2 - A_2$ (see Ref. 2 for the full expressions).

The angular brackets in Eq. (2) signify the effect of thermal broadening of the Fermi distribution on $\Delta\rho_{xx}$ and represent the factor $D(X)$ for the Δg_i. Coleridge identified the appropriate factor as $D(2X)$ for the term involving the product $\Delta g_1 \Delta g_2$, but this is incorrect because it does not include interference or resonance effects, as will be shown below. This term is described by the equation

$$\frac{\langle \Delta g_1 \Delta g_2 \rangle}{g_0{}^2} = 4\Phi(T_{D_1}+T_{D_2})\int_0^\infty \cos\left\{2\pi\frac{E-E_{01}}{\hbar\omega_c}+\pi\right\}\cos\left\{2\pi\frac{E-E_{02}}{\hbar\omega_c}+\pi\right\}\left\{-\frac{\partial F}{\partial E}\right\}dE \tag{4}$$

$$= 2\Phi(T_{D_1}+T_{D_2})\int_0^\infty \left\{\cos 2\pi\frac{2E-(E_{02}+E_{01})}{\hbar\omega_c}+\cos 2\pi\frac{E_{02}-E_{01}}{\hbar\omega_c}\right\}\left\{-\frac{\partial F}{\partial E}\right\}dE\ . \tag{5}$$

The second integral just returns $\cos\{2\pi(E_{02}-E_{01})/\hbar\omega_c\}$ and, using the results of Dingle[8] to evaluate the first integral analytically and setting $(E_F-E_{0i})/\hbar\omega_c = f_i/B$, this finally yields

$$\frac{\langle \Delta g_1 \Delta g_2 \rangle}{g_0{}^2} = 2\Phi(T_{D_1}+T_{D_2})\left\{D(2X)\cos 2\pi\frac{f_1+f_2}{B}+\cos 2\pi\frac{f_1-f_2}{B}\right\}. \tag{6}$$

Using this result, Eq. (2) (without the term in A_2 which is easily separated since $f_2 \ll f_1$) is replaced by

$$\frac{\Delta\rho_{xx}}{\rho_0} = 2A_1\Phi(T_{D_1})\left\{D(X)\cos\left[2\pi\frac{f_1}{B}+\pi\right]+\beta D(2X)\cos 2\pi\frac{f_1+f_2}{B}+\beta\cos 2\pi\frac{f_1-f_2}{B}\right\}, \tag{7}$$

where $\beta=(B_{12}/A_1)\Phi(T_{D_2})$.

As $T\to 0$ the components at $f_1 \pm f_2$ have equal magnitudes and we produce amplitude modulation of the component at f_1, with equal amplitude sidebands. As the temperature increases the component at f_1+f_2 is rapidly attenuated by $D(2X)$, e.g., by $X=2$, $D(2X)=0.15$; thus we will see mainly the components at f_1 and f_1-f_2. At even higher values of X, only the oscillations at f_1-f_2 remain. This behavior is basically in accord with the data in Refs. 2 and 3 and with our experiments presented in Sec. III. It seems clear that the numerical calculation that Coleridge[2] presented is also consistent with these ideas and did indeed show these interference effects.

The physical origin of the three terms of Eq. (2), and the reason why the component at f_1-f_2 behaves so differently, is of some interest. In the approximation that terms in n_2/n_1 are negligible, all the effects are due to oscillations in the conductivity of the lower subband. In the semiclassical model[2,7] the conductivity of this band is determined by the product of the effective number of electrons $n_1^{\text{eff}}=n_1(1+\Delta g_1/g_0)$ and the scattering probability $P_{11}(g_0+\Delta g_1)+P_{12}(g_0+\Delta g_2)$ which includes both intrasubband and intersubband scattering. The first term in Eq. (2) then arises from the oscillating parts of the product $n_1(1+\Delta g_1/g_0)P_{11}(g_0+\Delta g_1)$, the basic result for a single occupied subband, and $n_1(1+\Delta g_1/g_0)P_{12}g_0$, the additional contribution from intersubband scattering. For $P_{12}=0$ this yields $A_1=2$. The second term is from the product $n_1P_{12}\Delta g_2$ and so is seen to be caused by the scattering probability of the lower subband electrons being modulated by the oscillations in the density of states in the upper subband. Notice that the upper subband electrons make no contribution to the resistivity in this approximation. Both of these terms produce typical SdH oscillations which are primarily determined by the DOS of each of the Landau-level ladders at E_F. Because each term involves only a single set of Landau levels, it is damped by broadening of the Fermi function in the usual way to give a factor $D(X)$.[8]

The last term arises from the product $n_2P_{12}\Delta g_1\Delta g_2$ and so involves both sets of Landau levels. The interesting component at f_1-f_2 is not damped by temperature and arises because of a resonance effect between the Landau levels of the two subbands. The cosine terms in Eq. (4) are always in phase whenever $E_{02}-E_{01} = \text{integer}\times\hbar\omega_c$, i.e., the Landau levels for the two subbands are coincident. Under these conditions elastic scattering becomes resonant, and the conductivity of the lower subband always shows a maximum. The difference frequency arises because only the relative positions of the two sets of levels matters: the location of either set relative to E_F is not significant. The condition of elastic scattering means that the two sets of energy levels are always compared point by point on the energy scale, so there is no thermal smearing. The appearance of such resonant intersubband scattering has been reported by Leadley *et al.*[9] in single subband heterojunctions at higher temperatures, due to thermal population of higher Landau levels in both subbands.

III. EXPERIMENTS

The magnetoresistance of three heterojunctions has been measured at temperatures between 0.5 and 4.2 K in the magnetic-field range below 1.5 T. To increase the upper subband populating the samples were all photoexcited at 4.2 K with a red light-emitting diode until saturated and then left to settle until the resistivity was constant. The final carrier density varied slightly on different cool downs and so the data presented on each sample were taken in the same session, where no noticeable change occurred. Table I shows the relevant characteristics of the illuminated samples, grown by molecular-beam epitaxy at Philips Research Laboratories. Sample G590 was not measured below 1.1 K and so we will concentrate on data from samples G131 and G215. The general trends are similar for all three, with sample G590 resembling sample G215 most closely. The resistance was measured in two distinct regimes: (a) as a function of bath temperature using a sufficiently small current such that the electrons remained in thermal equilibrium with

TABLE I. Characteristics of the samples as measured in this study. L_z is the width of the undoped $Ga_{0.7}Al_{0.3}As$ spacer layer; μ is the mobility in the absence of magnetic field; n_1 and n_2 are the carrier densities in the lower and upper subbands deduced from f_1 and f_2, the frequencies of the two series of SdH oscillations at the lowest temperature; T_{D_i} and A_i are the respective Dingle temperatures and amplitudes for these series (see text for details); Ξ is the value of X at which a strong minimum appears in the modulation envelope of the oscillations at frequency f_1, and is tabulated for the cases of cold and hot electrons. The values of Ξ lie within the quoted error range for many sets of data, except those marked * where only one zero was found.

Sample	L_z (nm)	μ ($m^2/V\,s$)	n_1 (10^{15} m^{-2})	n_2 (10^{15} m^{-2})	f_1 (T)	f_2 (T)	T_{D_1} (K)	T_{D_2} (K)	A_1	A_2	Ξ Cold	Ξ Hot
G131	1.7	15.4	9.65	0.77	19.95	1.60	3.0±0.1	0.67±0.05	2.6±0.3	0.33±0.04	5.7*±1.0	7.8*±1.0
G215	10	54	7.57	0.52	15.65	1.08	1.1±0.1	0.55±0.05	2.6±0.5	0.32±0.06	6.6±0.5	6.5±1.0
G590	10	90	6.6	0.29	13.6	0.59	0.7±0.1	0.1±0.1	2.05±0.3	0.17±0.04	7.0±0.5	

the lattice—referred to as "cold" data; (b) heating the electrons out of equilibrium with the lattice, by increasing the measuring current, at the lowest bath temperature reached—"hot" data.

Direct current was used at all times to ensure consistency between hot and cold data. The amplified voltage was recorded digitally at equal intervals of $1/B$ to allow filtering by Fourier transform. The magnet used was an air cored solenoid with negligible hysteresis and a field accurately linear in current. The bath temperatures were measured with a calibrated Ge resistor with the sample in exchange gas. These temperatures did not vary by more than 30 mK over each data set.

A. Cold electrons

The magnetoresistance contains a number of components as follows (cf. Fig. 1): a slowly varying background, a high-frequency series of SdH oscillations associated with the lower subband, a similar series at a lower frequency associated with the upper subband, and a modulation of one series by the other.

Initially most of the background was removed by subtracting a low-order polynomial in B (with a much smaller curvature than the oscillations). Then the two series were separated using suitable pass bands in the Fourier transform. The high-frequency series could be completely isolated, but that at f_2 was at too low a frequency for complete isolation from the background.

The coefficients f_1 and T_{D1} relevant to the high-frequency series (see Table I) were obtained as follows. The oscillations are damped towards low field by both the thermal and Dingle factors of Eq. (1) and so in order to see the oscillations over the whole field range, the amplitude was first divided by $D(X)$ (using the bath temperature) and then $\Phi(T_{D_1})$, with T_{D_1} chosen to give a constant amplitude for the oscillations at the lowest temperature, ignoring the modulation. Examples of the resulting normalized oscillations are shown in Figs. 2(a) and 3(a) at various temperatures. The average amplitude of the low-temperature data (lower traces), of which there were several sets, was used to estimate A_1. (See Sec. IV for a better method of obtaining A_1.) In these data there is one dominant frequency f_1 which we associate with the lower subband and have evaluated by essentially fitting a series of integers to all the zero crossings on an inverse field scale, giving a maximum error in f_1 of $<0.2\%$.

There are fewer oscillations at f_2 and, because of the background separation problem, the above technique could not be used. Instead, A_2, f_2, and T_{D_2} were obtained by directly fitting all the low-frequency data, including the background, to Eq. (1) plus a polynomial in field including terms up to B^3. In this way f_2 was found to an accuracy of $\sim 2\%$. The phase constant of these oscillations, which was also a fitting parameter, was indeed found to be π to within the experimental error of 5%.

From the values of f_1 and f_2, the electron density in each band n_i can be calculated from $n_i = 2ef_i/h$. In each case n_1+n_2 agreed with the total electron density deduced from the high-field Hall coefficient to better than 1%, thus confirming the identity of f_1 and f_2.

If the lower subband oscillations were completely described by Eq. (1) they should show a constant amplitude when normalized, but several deviations can be clearly seen in Figs. 2(a) and 3(a) as follows:

(i) Modulation of the amplitude at the frequency of the upper subband oscillations, showing a minimum whenever there is a minimum in the series at f_2, i.e., E_F lies between upper subband Landau levels.

(ii) The appearance of particularly strong minima in this modulation. These only occur when X is close to a fixed ratio Ξ the value of which is weakly sample dependent (see Table I). If, at a particular temperature, the condition $X=\Xi$ is satisfied at one of the minima, then this minimum actually becomes zero and is the only strong feature in the modulation, otherwise there are two strong minima, at fields at either side of this condition.

(iii) For $X \ll \Xi$ the normalized amplitude is approximately constant at all lattice temperatures showing that the damping of the oscillations in this region is reasonably described by $D(X)$, using the bath temperature, and that a constant T_{D_1} is appropriate.

(iv) For $X > \Xi$ the normalized amplitude increases rapidly. This means that these low-field oscillations cannot be described as being sampled by $D(X)$. Indeed for sample G215 at 4.2 K the oscillations are more than four orders of magnitude larger at 5 T^{-1} than would be predicted using Eq. (1). In addition their phase differs continuously (relative to those at low X), indicating a frequency of $f_1 - f_2$ rather than f_1. (We will not present our phase plots here, but they are similar to those in Ref. 3.)

In contrast, fits to the low-frequency component (mentioned earlier) at all bath temperatures do not show any anomalies. By fixing A_2, T_{D_2}, and f_2 to the values obtained at low temperature, the data can be fitted leaving the electron temperature T as the only free variable (apart from the background which varies). For sample G131 the temperature so obtained is always within 0.1 K of the bath temperature, and considerably better than this below 3 K. Sample G215 has fewer oscillations at f_2 making the fits less definitive, but T is still found to be within 0.1 K of the bath temperature below 3 K, though this error increases to ~ 0.3 K by 4.2 K. Again the phase constant does not vary significantly from π, demonstrating that f_2 does not change with temperature.

The normalized high-frequency oscillations have been Fourier transformed, with the results shown in Figs. 4(a) and 5(a). The advantages over the original transform are that, if Eq. (1) is appropriate, equal weighting will now be given to oscillations at all fields, whereas previously the high-field oscillations dominated. There are two major points to notice. First, that as the temperature is in-

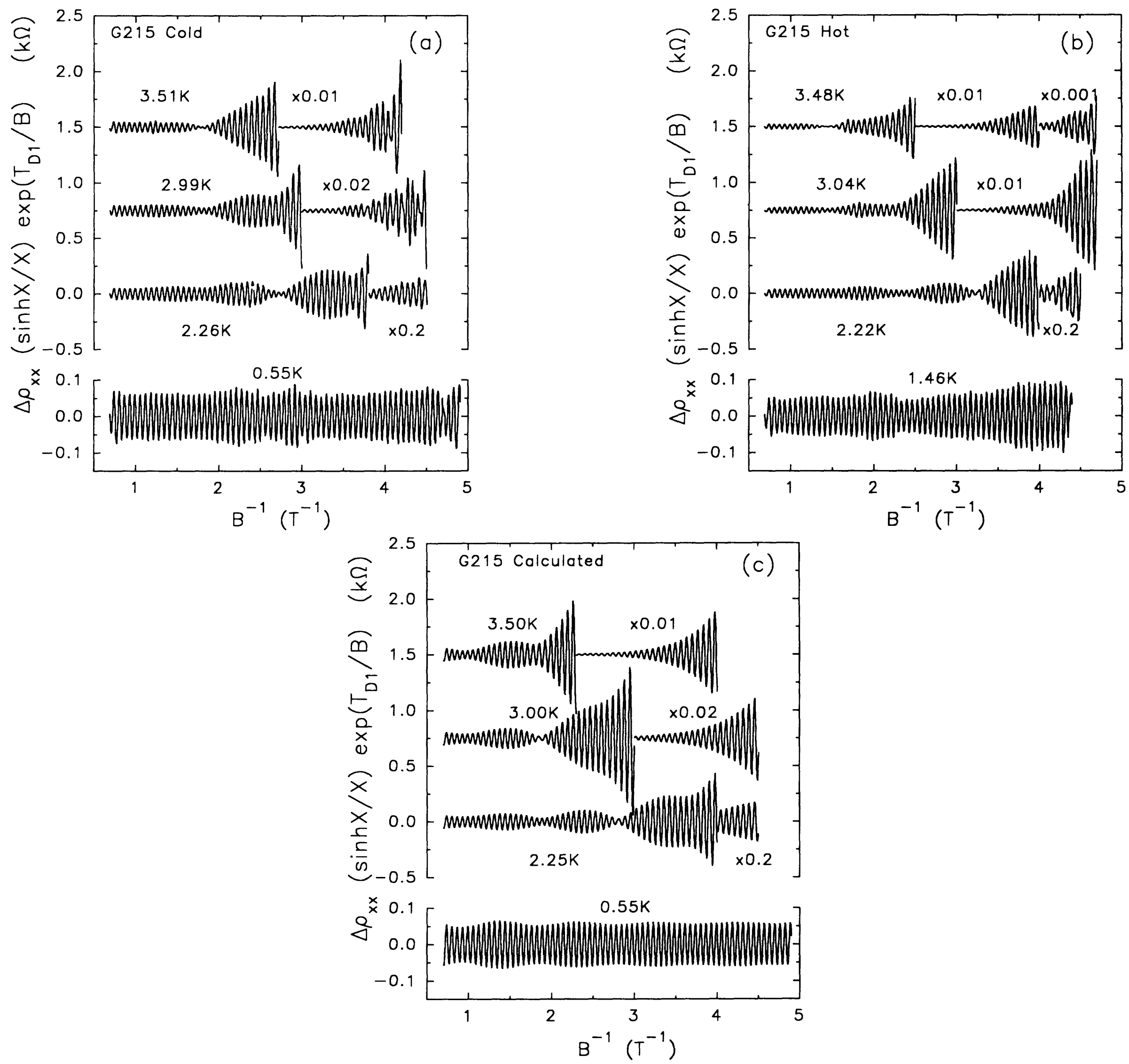

FIG. 2. The high-frequency oscillations, normalized by correcting for both the Dingle and thermal damping factors, as a function of inverse magnetic field for sample G215. In each case notice the scale change for the lowest trace. Data have been offset for clarity. (a) Experimental data for cold electrons. (b) Experimental data for hot electrons. The results are superficially similar to those in (a) but there are two major differences. (i) The modulation envelope has shifted in phase by π (relative to the component at f_2). (ii) In the region of anomalous amplitude growth (right-hand side of the upper traces) the phase of the individual oscillations differs from those in (a) by π, i.e., the amplitude has effectively reversed sign. (c) Results calculated using the same nominal temperature as in (a). There are no adjustable parameters. We have used $A_1 = 2.0$ and $B_{12} = A_2$, with the value of A_2 taken from Table I.

creased the peak at $f_1 - f_2$ grows compared to that at f_1. This is due to the oscillations referred to in (iii) above becoming relatively more important as they dominate over more of the field range and confirms their frequency very accurately. Second, that at all but the lowest temperature there is no visible feature at $f_1 + f_2$ as would be expected for simple amplitude modulation of f_1 by f_2.

B. Hot electrons

The magnetoresistance was also measured at a fixed lattice temperature of 0.5 K (1.15 K for sample G590), using current of up to 40 μA to heat the electrons out of thermal equilibrium. Electron temperatures were obtained by fitting the component at f_2 as outlined above. The resulting normalized high-frequency oscillations are shown in Figs. 2(b) and 3(b). The results are similar to those for cold electrons, but closer inspection reveals that the phase of the modulation is shifted and that for hot electrons the modulation envelope has minima where the low-frequency oscillations have maxima, while for cold electrons the reverse was found. Although all the data from samples G215 and G590 exhibit these phase shifts for hot and cold electrons, the picture is somewhat different for sample G131, where the elastic impurity scattering is stronger. For the hot-electron case at lower electron temperatures [cf. the trace at 2.87 K in Fig. 3(b)] the modulation envelope has the same phase as for cold electrons. But in the hottest data [the trace at 5.34 K in Fig. 3(b)] the phase has shifted just as for the other two samples. In the regions where the oscillations at $f_1 - f_2$ dominate, the phase of the individual oscillations is also

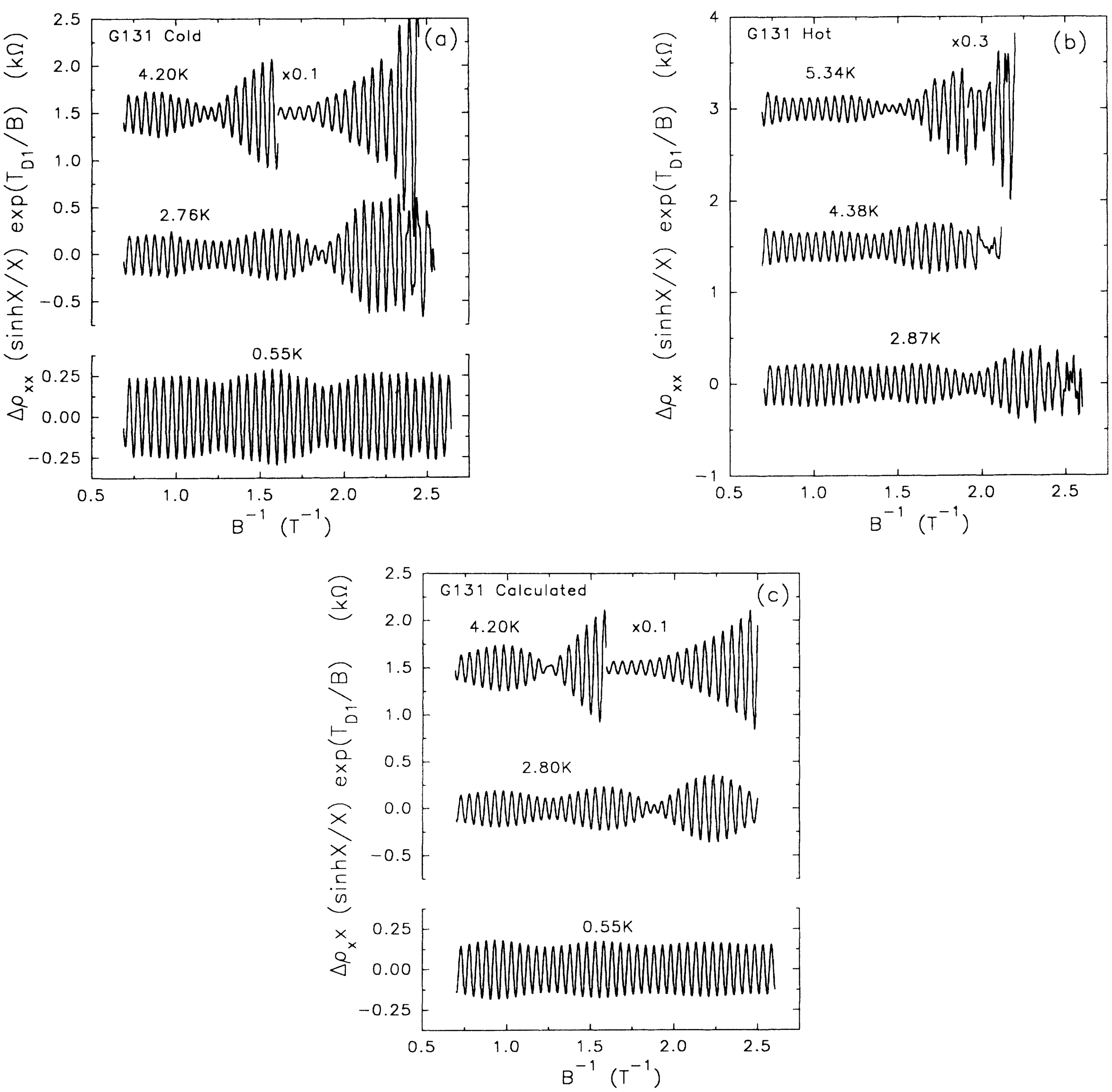

FIG. 3. Similar to Fig. 2, but for sample G131. The comments in the caption to Fig. 2 still hold. However notice that in (b) the modulation minimum at 2.87 K is still close to the position seen for cold electrons, but by 5.34 K the minimum has shifted by π. The phase of the oscillations at fields below this latter minimum has also changed by π.

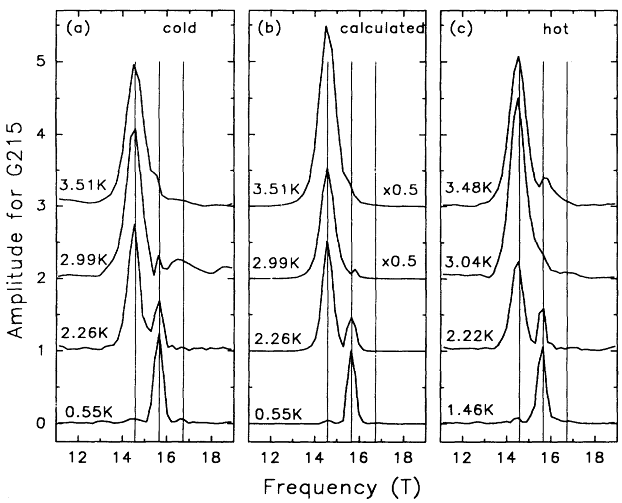

FIG. 4. Fourier transforms of the data for sample G215 shown in Figs. 2(a)–2(c). Transforms at different nominal temperatures are offset vertically for clarity. The thin vertical lines at 14.57, 15.65, and 16.73 T correspond to f_1 and $f_1 \pm f_2$. Notice that at higher temperatures there is no visible feature at f_1+f_2. The width of the peak at f_1 is determined only by the finite range of the original data and the apodization used in taking the transforms. The peak at f_1-f_2 is always wider because, in the normalized data of Fig. 2, the component at f_1-f_2 increases exponentially as $1/B$ increases. The amplitudes of the transforms are on an arbitrary scale. Data sets at the same nominal temperature have been truncated to identical end points of magnetic field before transforming. Thus the relative amplitudes of such a trio may be quantitatively compared (but note the scale factors of $\times 0.5$).

shifted by π compared to the case for cold electrons.

For sample G215 the values obtained for Ξ with hot electrons are the same as those for cold electrons at 6.5 ± 1, though a trend from larger to smaller values is noticeable as the heating increases. For sample G131 the single clear modulation zero gives $\Xi=7.8\pm1$ which is higher than that for cold electrons at 5.7 ± 1.

Fourier transforming these data again shows the increase in intensity of the peak at f_1-f_2 compared with that at f_1 at higher electron temperatures [Figs. 4(c) and 5(c)].

IV. DISCUSSION

In common with Coleridge we are unable to detect any temperature variation in the magnitude of A_2 for samples G215 and G131 over the range 0.5–4 K (Fig. 6). Table I gives our mean values. There are too few oscillations resolved at f_2 in sample G590 to make this a valid exercise except at the lowest temperatures ($1.1 < T < 2.0$ K). The values are similar to the 0.35 obtained by Coleridge for a single sample, although they show some variation which is not clearly correlated with the sample properties. The estimates are roughly in line with those obtained by Leadley *et al.*,[10] using the change of resistivity on depopulation of the upper subband by a magnetic field parallel to the plane of the 2DEG.

The primary interest of the present paper is in the origin of the modulation effects, which in the above model appear in the last term of Eq. (2), and it is interesting that there are essentially no new unknowns since $B_{12} \simeq A_2$. Our high-frequency data have been filtered to remove oscillations at f_2 and the results should be approximately represented by Eq. (7). Figures 2 and 3 compare the results of evaluating this equation, using $A_1=2.0$ and $B_{12}=A_2$, with our normalized experimental results. The agreement is very good, especially for sample G131. The calculation gives not only reasonable values of the amplitudes, but also places the modulation minima at the correct locations. A closer examination does, however,

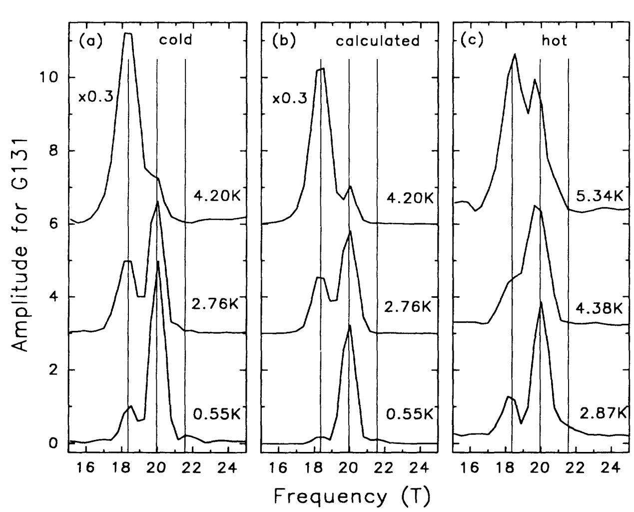

FIG. 5. Fourier transforms of the data for sample G131 shown in Figs. 3(a)–3(c). The caption of Fig. 4 is still appropriate, except that the hot data in 4(c) had to be truncated to a slightly smaller range than in 4(a) and 4(b). The values of f_1 and $f_1 \pm f_2$ are now 18.35, 19.95, and 21.55 T.

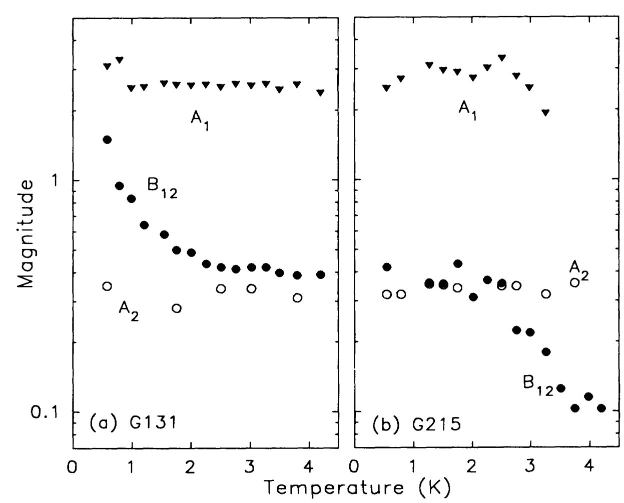

FIG. 6. Magnitudes of the coefficients A_1 and B_{12} as a function of temperature deduced from comparisons of the experimental and calculated transforms, as described in the text, for (a) sample G131 and (b) sample G215. The values of A_2 found by fitting the low-frequency oscillations are included for comparison.

yield some discrepancies in the details, particularly for sample G215 at higher temperatures.

More quantitative comparisons can be made between theory and experiment by using the Fourier transforms to obtain magnitudes of A_1 and B_{12} as a function of temperature. The amplitudes of the peaks at f_1 and f_1-f_2 were converted to absolute values of A_1 and B_{12}, respectively, by scaling the transforms of the experimental data using transforms of calculated data. These latter data were calculated at the same temperature, over exactly the same range of magnetic field and contained the same number of data points. The results for A_1 and B_{12} are shown in Fig. 6. The calculated and experimental transforms of Figs. 4 and 5 show that the data from sample G131 are always reasonably reproduced whereas those from sample G215 are again most accurate at lower temperatures. The dominance of the component at f_1 at low X, and the component at f_1-f_2 at high X, can be inferred from the change in amplitude with temperature of the relevant peaks in the transforms, though this is most clearly seen in the phase plots of Ref. 3. In both samples the component at f_1+f_2 (which could, in principle, also provide a value for B_{12}) is not significant in either the calculated or experimental results, except at the very lowest temperatures as expected.

In both samples G131 and G215 there is no visible change of A_1 with temperature. This shows that the damping factor $D(X)$ accurately describes the behavior of this component, as was found to be the case for A_2 earlier. It also shows that there is no significant variation in T_{D_1} with temperature. The average values for A_1 for these two samples are identical at 2.6 (± 0.3 for sample G131 and ± 0.5 for sample G215), and are larger than the expected value of $2-A_2 \simeq 1.7$.

The coefficient B_{12} is expected to be close to A_2 and over part of the temperature range this is found to be so for both samples (Fig. 6). However, the range of good agreement is different for each. For sample G131 the range extends from 2–4.2 K, with B_{12} being 0.41 ± 0.04 compared with a value of 0.33 ± 0.04 for A_2. For this sample B_{12} rises continuously below 2 K. This has little effect on the agreement between the calculated and experimental wave forms of Fig. 3 because at low temperatures these are dominated by the component at f_1. It is possible that the variation of the Fermi level with field (which is most pronounced at low temperature, but not included in the calculation) will affect the relative magnitudes of the components at $f_1 \pm f_2$, and it seems to be true that the component at f_1+f_2 [Fig. 5(a) bottom trace] is in better agreement with the calculated amplitude [Fig. 5(b)]. Nevertheless, this increase is not observed for sample G215 and so its origin remains unknown.

On the other hand, the value of B_{12} for sample G215 agrees well with A_2 at low temperatures, but shows a rapid drop in magnitude for $T \geq 2.5$ K. This decrease for sample G215, but not for sample G131, is consistent with the following observed behavior of the samples. At a zero in the modulation the first and third terms of Eq. (7) have equal amplitudes (ignoring the middle term which we have shown to be negligible at elevated temperatures). This will happen when $D(X) \simeq \beta$. For sample G131, using the experimental values of T_{D_2}, A_1, and A_2 from Table I, this predicts that at $B^{-1} \sim 1.9$ T^{-1}, the zero in the modulation should occur at $T \sim 3.0$ K, which it actually does. However, in the higher mobility samples there are discrepancies, e.g., for sample G590, $D(X)=\beta$ is satisfied for $X \sim 4.7$, in contrast to the experimentally observed value of ~ 7.0. This indicates that the calculated value of the resonance term is too large in the high mobility samples, especially at high temperatures.

It is clear that the main features of the experimental data for cold electrons are well reproduced by the theory. Nevertheless it is also clear that the theory is unable to account for the phase shifts of the modulation maxima and minima that are seen for hot electrons, especially for the two higher mobility samples. Such a phase change implies that the oscillation at f_1-f_2 is now represented by $\cos(2\pi\{f_1-f_2\}/B+\pi)$, i.e., there is an extra phase factor of π compared with Eq. (7). Indeed if the experimental data for hot and cold electrons are superposed at high X the phase difference in the component at f_1-f_2 is clearly seen. This is a very dramatic change and, following similar arguments as in Sec. II, means that the positive peaks in the oscillations at f_1-f_2 now occur when the two Landau-level ladders are exactly interleaved. Because these effects are not predicted in the elastic-scattering theory, we presume that their origin is to be found in a mechanism for which inelastic scattering plays a dominant role.

This identification is also consistent with the general trends seen in samples G131 and G215. Thus the higher mobility sample G215 shows the rapid fall in B_{12} at high temperature in the cold-electron case, but a similar fall is not seen for the lower mobility sample. This suggests that there is a competition between inelastic and elastic effects (which give rise to oscillations with opposite phases) and hence partial cancellation of the component at f_1-f_2. Similarly, in the hot-electron case, sample G131 shows the phase shift in the modulation, relative to the cold case, but only at higher temperatures whereas samples G215 and G590 always show this phase shift; this is all clearly consistent with elastic effects being stronger for sample G131 as we might expect. In view of the energy emitted or absorbed in an inelastic-scattering event, it is perhaps not surprising that the interleaving of the Landau levels might be the condition required to maximize inelastic intersubband scattering. (This might be roughly comparable to the single-band case,[11] where inelastic inter-Landau-level scattering is maximized when the Fermi level is midway between two Landau levels.)

It is surprising that inelastic scattering should be so important in the temperature region below 4 K, where it only affects the mobility weakly. Experiments by Harris *et al.*[4] show that by 4.2 K the contribution of acoustic-phonon scattering to ρ_0 could be as much as 5% for sample G215, while it will only be $\sim 1\%$ for sample G131. This is quite consistent with our observations that deviations from the elastic-scattering model are much greater for sample G215. The coefficient A_2, which is primarily a measure of the intersubband scattering rate from lower to upper subband, is not visibly temperature dependent, though we would not see changes of less than 10%. It is worth mentioning that the inelastic-intersubband-scattering process is quite sharply defined in terms of energy due to the conservation of momentum. This serves to narrow the effective energy range to ~ 2 K and so reduces much of the effect of temperature on this type of scattering. A further possibility, specific to the hot-electron configuration, is that the energy-loss rate may oscillate with magnetic field, resulting in variations in the electron temperature. Since the background resistivity has a weak temperature dependence, this could give rise to oscillations in the resistivity. It remains to be seen whether a detailed theory combining elastic and inelastic scattering can successfully explain all the observations.

V. CONCLUSION

For electrons in thermal equilibrium with the lattice, the measured oscillations in the magnetoresistance are well described by the elastic intrasubband and intersubband model of Coleridge, especially when applied to the lower mobility sample G131. The strong modulation effects that are seen are caused by another series of oscillations which, at all but the lowest temperatures, are dominated by a component at the difference frequency $f_1 - f_2$. Contrary to Coleridge's conclusion, this series is not thermally damped in the manner normally appropriate to the Shubnikov–de Haas oscillations. This is because the new oscillations are due to a resonance between the two sets of Landau levels. The strength of the resonance is determined only by the ratio of the combined Landau-level broadenings to the cyclotron energy, as embodied in the product of Dingle terms that appears in Eqs. (6) or (7). This resonance has many features which are similar to the phenomenon of magnetophonon resonance (MPR), although in the latter case only a single Landau-level series is involved. MPR occurs because the relevant optic-phonon energy $\hbar\omega_{LO}$ is sharply defined so that only electron states differing in energy by $\hbar\omega_{LO}$ can take part in the scattering. Correspondingly, in the present intersubband scattering, only states at the same energy in the two subbands are bridged by elastic scattering. In both cases the resonance is not reduced when the Fermi function is broadened beyond $\hbar\omega_c$. By contrast, the usual Shubnikov–de Haas oscillations are sharpest at the lowest temperatures and become strongly damped when the Fermi function broadening is similar to $\hbar\omega_c$.

The model becomes less successful as the temperature rises for cold electrons, especially for the high mobility samples. It also fails dramatically for hot electrons. In the latter case, the predictions are superficially correct but the phase change of π seen for the component at $f_1 - f_2$ cannot be explained. Interestingly a π phase change is also associated with hot-electron MPR.[9] In the present case we conclude that the deficiencies in the model are due to the neglect of inelastic-scattering effects which become increasingly important for cold electrons as the temperature is raised, and appear to dominate for hot electrons at all temperatures in the higher mobility samples.

ACKNOWLEDGMENTS

The authors would like to thank Philips Research Laboratories, Redhill, Surrey RH1 5HA, UK, for providing the samples. D.R.L. was supported by the Rutherford Appleton Laboratory, Chilton, Didcot, Oxon. This work was supported in part by the Natural Science and Engineering Research Council of Canada. R.F. would also like to thank the Royal Society (London) for financial assistance during a stay in Oxford.

---

*Permanent address: Department of Physics, Queen's University, Kingston, Ontario, Canada K7L 3N6.

[1] D. R. Leadley, R. J. Nicholas, J. J. Harris, and C. T. Foxon, Semicond. Sci. Technol. **4**, 885 (1989).

[2] P. T. Coleridge, Semicond. Sci. Technol. **5**, 961 (1990).

[3] R. Fletcher, J. J. Harris, and C. T. Foxon, J. Phys. Condens. Matter **3**, 3479 (1991).

[4] J. J. Harris, C. T. Foxon, D. Hilton, J. Hewitt, C. Roberts, and S. Auzoux, Surf. Sci. **229**, 113 (1990).

[5] T. Ando, J. Phys. Soc. Jpn. **37**, 1233 (1974).

[6] A. Isihara and L. Smrcka, J. Phys. C **19**, 6777 (1986).

[7] P. T. Coleridge, R. Stoner, and R. Fletcher, Phys. Rev. B **39**, 1120 (1989).

[8] R. B. Dingle, Proc. R. Soc. London Ser. A **211**, 517 (1952).

[9] D. R. Leadley, M. A. Brummell, R. J. Nicholas, J. J. Harris, and C. T. Foxon, Solid State Electron. **31**, 781 (1988).

[10] D. R. Leadley, R. J. Nicholas, J. J. Harris, and C. T. Foxon, Semicond. Sci. Technol. **5**, 1081 (1990).

[11] L. J. Challis, A. J. Kent, and V. W. Rampton, in *High Magnetic Fields in Semiconductor Physics II,* edited by G. Landwehr (Springer, New York, 1989), p. 529.